Natural Hazards
and Earth System
Sciences
Discussions

Open Access

Coastal flooding of urban areas by overtopping: dynamic modelling application to the Johanna storm (2008) in Gâvres (France)

S. Le Roy[1], R. Pedreros[1], C. André[1,2], F. Paris[1], S. Lecacheux[1], F. Marche[3], and C. Vinchon[1]

[1]BRGM, 3, avenue Claude Guillemin, BP 36009, 45060 Orléans Cedex 2, France
[2]LETG-Brest Géomer, UMR 6554 CNRS, University of Western Brittany, European Institute for Marine Sciences, Place Nicolas Copernic, 29280 Plouzané, France
[3]I3M, University of Montpellier 2 and INRIA LEMON, CC 051, 34000 Montpellier, France

Correspondence to: S. Le Roy (s.leroy@brgm.fr)

4947

Abstract

Recent dramatic events have allowed significant progress to be achieved in coastal flood modelling over recent years. Classical approaches generally estimate wave overtopping by means of empirical formulas or 1-dimensional simulations, and the flood is simulated on a DTM (Digital Terrain Model), using soil roughness to characterize land use. The limits of these methods are typically linked to the accuracy of overtopping estimation (spatial and temporal distribution) and to the reliability of the results in urban areas, which are places where the assets are the most crucial.

This paper intends to propose and apply a methodology to simulate simultaneously wave overtopping and the resulting flood in an urban area at a very high resolution. This type of two-dimensional simulation presents the advantage of allowing both the chronology of the storm and the particular effect of urban areas on the flows to be integrated. This methodology is based on a downscaling approach, from regional to local scales, using hydrodynamic simulations to characterize the sea level and the wave spectra. A time series is then generated including the evolutions of these two parameters, and imposed upon a time-dependent phase-resolving model to simulate the overtopping over the dike. The flood is dynamically simulated directly by this model: if the model uses adapted schemes (well-balanced, shock-capturing), the calculation can be led on a DEM (Digital Elevation Model) that includes buildings and walls, thereby achieving a realistic representation of the urban areas.

This methodology has been applied to an actual event, the Johanna storm (10 March 2008) in Gâvres (South Brittany, in western France). The use of the SURF-WB model, a very stable time-dependent phase-resolving model using NLSW equations and well-balanced shock-capturing schemes, allowed simulating both the dynamics of the overtopping and the flooding in the urban area, taking into account buildings and streets thanks to a very high resolution (1 m). The results obtained proved to be very coherent with the available reports in terms of overtopping sectors, flooded area, water heights and chronology. This method makes it possible to estimate very precisely not only the

4948

overtopping flows, but also the main characteristics of flooding in a complex topography like an urban area, and indeed the hazard at a very high resolution (water heights and vertically integrated current speeds).

The comparison with a similar flooding simulation using a more classical approach (a Digital Terrain Model with no buildings, and a representation of the urban area by an increased soil roughness) has allowed the advantages of an explicit representation of the buildings and the streets to be identified: if, in the studied case, the impact of the urbanization representation on water heights does indeed remain negligible, the flood dynamics and the current speeds can be considerably underestimated when no explicit representation of the buildings is provided, especially along the main streets. Moreover, on the seaside, recourse to a time-dependent phase-resolving model using non-stationary conditions allows a better representation of the flows caused by overtopping.

Finally, this type of simulation is shown to be of value for hazard studies, thanks to the high level of accuracy of the results in urban areas where assets are concentrated. This methodology, although it is currently still quite difficult to implement and costly in terms of calculation time, can expect to be increasingly resorted to in years to come, thanks to the recent developments in wave models and to the increasing availability of LiDAR data.

1   Introduction

Recent events have highlighted the exposure of human society to coastal flooding caused by cyclones or storm events. For example, Hurricane Katrina (2005) in Louisiana, Xynthia storm (2010) in France or Hurricane Sandy (2012) in the New York metro area left, in their wake, thousands of victims and billions of dollars' worth of damage to the built environment and economic losses, largely the result of marine flooding. Much recent effort has been devoted to improving numerical simulations of coastal flooding, in order to ensure communities have access to precise and relevant

knowledge about past and future hazards and to extrapolate from these the damage they may need to contend with in future.

Modelling flood dynamics in urban areas is a subject addressed quite recently; considerable headway has indeed been made in the field over the past decade, due to the need for fluvial flood simulations. Most commonly used methods developed to represent floods in urban areas rely on the same approach as for rural areas: the impact of the built environment is integrated by assigning high roughness coefficients at the scale of the urban area or of the building aggregates (for example, Gallegos et al., 2009, on a dam-failure case). Nevertheless, these methods do not enable a realistic representation of the flows in these zones of particular interest to be obtained.

The development of airborne scanning laser altimetry (LiDAR) has allowed floods to be simulated at a very high resolution, including urban areas, through different representations of individual buildings (inclusion as blocks in the topography, external walls, porosity, raised roughness, etc.). Schubert et al. (2008, 2012) tested different types of representation for the buildings (hole in the calculation grid, block, higher friction, porosity) with the BreZo model (Begnudelli et al., 2008), which uses unstructured meshes. The authors conclude that all these methods are able to represent the flood extension accurately provided the resolution is high enough, but that the flow velocities are harder to predict and more dependent on the method.

The resolution required must correlate with the sizes of buildings and streets. Neal et al. (2009) compared measurements taken after the 2005 Carlisle flood (UK) to simulations made with the LISFLOOD-FP model (Bates and De Roo, 2000; Bates et al., 2010) on a 25 m resolution DTM (Digital Terrain Model) and DEM (Digital Elevation Model). They conclude that at this relatively coarse resolution, it is better to use DTM than DEM to avoid water blockage by an aggregation of buildings. In order to estimate the appropriate resolution, Fewtrell et al. (2011) used terrestrial LiDAR data to simulate, with the same model, the flood that affected Alcester (UK) in 2007, compared the simulation results at very high resolutions (0.5, 1, 2 and 5 m), and concluded that, in this case, there is a gap, in terms of performance, between 2 and 5 m resolutions.

However, the critical resolution does remain specific to the numerical schemes of the model and to the site (width of the streets and of the buildings, orientation of the streets compared to the numerical schemes, etc.).

Coastal flooding brings up another question about the dynamics of incoming water, depending on state of the sea. Two main processes of coastal flooding are typically distinguished: the general overflowing (elevation of the sea level above protective structures or natural defences, caused by the combined effects of the tide, storm surge, and occasionally the wave setup) and the wave overtopping (passing of the waves above protective structures or natural defences). These two mechanisms are often coupled, with variable contributions and with a particular interaction caused by potential damage to the protections by wave shocks.

Urban coastal floods continue to be less frequently studied than continental flooding. Existing coastal flooding simulations usually concern generalized overflowing for the most part, for which broader areas are affected and waves can be neglected. The most common approach consists in imposing sea level (taking into account tide, storm surge and occasionally wave setup) on a coarse DTM, with a particular attention devoted to coastal defences. Urbanization is then represented by introducing a higher roughness coefficient, as for continental flood simulations at large scales. The models used are generally "storage cell" models (for example Bates et al., 2005) and NLSW (Non Linear Shallow Water) equations models (for example Fortunato et al., 2013; Gallien et al., 2011). Other simplified methods that do not entail the use of actual simulations proper consist in using static or semi-static methods to estimate the extent of the flooded area (Breilh et al., 2013).

The problem of coastal flooding due to wave overtopping is as yet imperfectly resolved. Most of the studies described in the scientific literature call on empirical formulations to estimate overtopping over the defences, like the TAW formulas (van der Meer, 2002). The flood simulation is then achieved via hydrodynamic models. Indeed, Smith et al. (2012) used the LISFLOOD-FP model on a 50 m-resolution DTM, combined with roughness to represent soil-use, to simulate a flood by combined surge and waves:

4951

the overtopping was represented by source cells where the overtopping rate had been estimated. On the site of Gâvres (Brittany, France), studied hereinafter, Le Cornec and Peeters (2008) used the TAW formulas on four profiles to estimate overtopping flows, and then used a hydrodynamic model to simulate the flood.

Recent progress in numerical methods has materially improved the approaches available in terms of wave overtopping simulations, allowing time-dependent phase-resolving models to acquire the requisite reliability. These models commonly use vertical integrated approaches, using either Boussinesq equations (dispersive, adapted to offshore propagation) or non-linear shallow water (NLSW) equations (non-dispersive, adapted to long waves).

Most of these recent models have adopted similar strategies to correctly represent the complex phenomenon of wave overtopping:

- shock capturing schemes have been implemented to simulate the steep wavefront in the surf zone; they allow the models to deal with highly variable flows and to treat discontinuities in the flows. Initially used to deal with broken waves, shock capturing schemes have proven very useful to simulate flows in very complex topographies such as urban areas (this type of scheme is now used for continental flooding simulations as well);

- well-balanced schemes were integrated to accommodate the sharp pressure gradients caused by steep slopes in the topography; these schemes, based on the equilibrium between source terms and velocity gradients, confer more stability to the model and allow it to converge towards an equilibrium state; here too, this characteristic developed for wave models has proven very convenient to simulate flows between buildings in urban areas;

- wave breaking needs specific processing to characterize energy dissipation and wave behaviour before and after breaking. It generally requires the identification of the breaking zone (geometrical or dynamical criteria). Subsequently, several strategies are used: Boussinesq models add a dissipation term to characterize

4952

the loss of energy (for example Lynett, 2006, 2010), while shock-capturing NLSW models are able to represent the behaviour of breaking waves (Bonneton, 2007; Brocchini and Dodd, 2008; Kobayashi et al., 1989; Marche et al., 2007). Another robust and elegant solution consists in using Boussinesq equations offshore, then identifying the breaking point and switching to NLSW equations to represent broken waves. This approach is seeing increasingly use (Tissier et al., 2012; Shi et al., 2012; McCabe et al., 2013; Tonelli and Petti, 2013), but it needs specific adaptations in terms of equations and numerical schemes (Bonneton et al., 2011; Lannes and Marche, 2014).

Currently, the operational use of these models is still limited mainly to 1-D simulations to estimate overtopping rates over coastal dikes (for example McCabe et al., 2013; Torres-Freyermuth et al., 2012; Lynett et al., 2010), or to 2-D simulations on experimental cases (for example, Tissier et al., 2012; Shi et al., 2012; Zijlema et al., 2011). Nevertheless, this recent progress, together with the availability of very high resolution topographic data, now allows such simulations in 2-D to be performed with very realistic conditions to estimate the conditions of coastal flooding as accurately as possible.

The choice of the overtopping and flooding model depends on the constraints of the site being studied. These include more particularly the position of the forcing conditions (conditioned by the numerical and physical limits of the models), the tidal context (duration of wave overtopping generally controlled by the tide in macro-tidal context, so the model must be robust enough to allow an overall variation in sea level to be simulated) and the domain characteristics (well parallelized models can counterbalance the lengthy computation time entailed when the area covered is extensive and the resolution needed is high).

The present paper proposes and applies a methodology to simulate coastal flooding by wave overtopping in an urban area, at a very high resolution. A simulation of a flood event induced by overtopping during the Johanna storm (2008) in the village of Gâvres (South Brittany, France) is conducted implementing this methodology and validated by

observations. This methodology can be adapted, or even simplified, to simulate coastal flooding due to generalized overflowing.

2   Modelling method

The proposed modelling process to simulate coastal flooding caused by a storm at very high resolution in urban areas (but likewise valid for rural areas), includes non-stationary conditions to estimate as realistically as possible (spatial distribution of the overtopping, chronology . . .) the water volume passing inland by wave overtopping and/or general overflowing. The overall method is illustrated on Fig. 1.

The method relies on prerequisite calculations at regional and local scales of the offshore characteristics of the storm:

(1) : a hydrodynamic free-surface model is used at a regional scale to simulate the sea level variations caused by both tide and storm surge. Several nested grids can be used to obtain a satisfactory resolution around the studied area, according to the scale of phenomena addressed. Typical models that can be used for this step are barotropic hydrodynamic models.

(2) : the waves are simulated by a spectral model that manages both generation by the wind and propagation of the waves. This simulation takes into account the evolutions of sea level and currents calculated in the previous simulation (*B*). Several nested grids are generally needed to achieve a sufficient resolution (a few meters or tens of meters) to account for the phenomena near the coast (especially wave breaking).

(3) : the last step is the simulation of the wave overtopping and associated flood, performed at very high resolution. This simulation includes the previous results (sea-level and wave characteristics) to represent the flood dynamics as realistically as possible. The use of an adapted model makes it possible to take land

use into account, especially in urban areas (interactions between flows and buildings). This is carried out using a DEM (Digital Elevation Model), based on LiDAR acquisitions, with an adapted resolution (determined by the size of streets, walls, inter-building spaces, etc.).

5   The application of this methodology to the flood caused by the Johanna storm (2008) in the village of Gâvres (South Brittany, France) is presented in the following paragraphs, with special attention devoted to the third phase, which is the most innovative.

3   Application to the Johanna storm in Gâvres

3.1   Study area, actual event and earlier work

10   The village of Gâvres is located on a small peninsula of South Brittany (France) adjoining the Lorient harbour exit. The site is exposed to a semi-diurnal macro-tidal context, with a maximum astronomic tidal range of 5.39 m (at Port-Louis; SHOM, 2012). The village centre is directly exposed to the waves coming from the Bay of Biscay to the south, with a limited protection offered by Groix island, located more than 7 km to the south-

15   west. Owing to its particular situation, Gâvres has suffered repeatedly from coastal flooding (1978, 2001, 2004, 2008, 2009, etc.), affecting mostly the lowest area, around the football pitch, that is known to be a former wetland that has been polderized and urbanized since the fifties (Cariolet, 2011).

The event studied in the present paper occurred on 10 March 2008, caused by the

20   Johanna storm. This storm, described by Cariolet et al. (2010), struck Brittany and areas northwards; the trajectory of the depression passed over southern Ireland and England from west to east, with atmospheric pressures reaching 975 hPa in extreme western Brittany, maximum winds of 150 km h^{-1} and significant wave heights exceeding 13 m. The coincidence of the generated storm surge (between 0.7 and 0.8 m measured

25   in South Brittany) with a period of spring tides caused considerable damage due to

4955

scattered coastal flooding extending from South Brittany to Normandy and Picardy (André et al., 2013; André, 2013).

In Gâvres, the two successive high tides of 10 March 2008 (05:11 and 17:22 in Port-Tudy[1]) led to wave overtopping over the dike of the main beach and subsequent

5   flooding in the village, mostly during the morning high tide. Figure 2 illustrates the general phenomena in Gâvres, with overtopping waves coming from the south. According to witnesses (Le Cornec and Peeters, 2008), the lowest topographic point of the area was reached by water at about 05:00 and the level rose until approximately 06:00 to reach more than 1 m high (Cariolet, 2010). No available data enables us to estimate

10   the duration of the overtopping and the evolution of the incoming flow rate during the storm.

Le Cornec and Peeters (2008) have applied a methodology developed and validated by Peeters et al. (2009) to simulate this event using a simulation of wave generation and propagation, by a spectral model (Mike 21 SW), some 1-D simulations of the wave

15   climate propagation along four profiles, with a one-hour time step. This allowed the estimation of the wave characteristics on the dike (model LITPACK), an estimation of the hourly overtopping flows over the dike (on the four profiles) through empirical formulas of the TAW (van der Meer, 2002), and finally a simulation of the flows with an hydrodynamic model (Mike 21 HD) at a 2.5 m resolution. Their results correspond

20   closely to reports and measurements, despite a slight overestimation of the flood (in extension and water heights). The methodology proposed in the present paper aims, in particular, to improve the modelling of the overtopping processes.

---

[1]In the remainder of this paper, all the indicated hours are UTC, for both the actual event and simulations.

4956

3.2 From the regional scale to the local scale

3.2.1 Modelling the sea level evolutions: tide and storm surge

The simulation of the sea level evolutions has been conducted with the MARS model, developed by Lazure and Dumas (2007). The calculations were applied to two regular nested grids having resolutions of 2 km and 400 m respectively (the calculation domains are depicted on Fig. 2). The larger grid was used to calculate the atmospheric storm surge. On the nested grid, the tide was simulated by the forcing on the boundaries of the calculation domain of this storm surge combined with 143 tidal components supplied by SHOM (database CST France, Le Roy and Simon, 2003). To simulate the storm surge, the atmospheric conditions are derived from the CFSR-NOAA dataset (Saha et al., 2010): winds and atmospheric pressure, available at a 0.5° resolution, were exploited to calculate the non-stationary sea level over the whole studied area, and during a long enough period to attain an established situation. The results turn out to be very coherent with the observations available for the 10 March 2008 in terms of total sea level and of storm surge, especially in Port-Tudy (Groix island, Fig. 3) and Concarneau, where the nearest available tide gauges are located.

According to the simulation (left-hand portion of Fig. 3), the maximum storm surge near Gâvres exceeded 70 cm from about 04:20 through 05:00. The simultaneity of this maximum surge with the high tide (05:20) is the main explanation for the flood in Gâvres on this day: it led to a maximum sea level of 3.13 m above mean sea level at 05:10 (i.e., 55 cm higher as compared to the highest astronomic tide).

3.2.2 Modelling the waves

The waves were simulated by means of the two-dimensional spectral model SWAN (Booij et al., 1999). To do so, two nested grids were used, with respective resolutions of 166 m and 10 m in the coastal area (calculation areas on Fig. 2). The model was forced with the waves spectra calculated in the IOWAGA project (Ardhuin et al., 2010), by

the wind drawn from the CFSR-NOAA dataset (Saha et al., 2010) and by the currents and sea levels from the previous simulation (MARS model). The IOWAGA simulations appear to be reliable for the Johanna storm, as illustrated on Fig. 4 for the Pierres-Noires gauge (western extremity of Brittany). The non-stationary simulation covers the period from the 9 to 11 March 2008.

This makes it possible to simulate the evolution of the waves that affected Gâvres, in terms of spectra and of overall characteristics (significant height, period, direction, setup, breaking, etc.). The results show that at the peak of the storm (about 05:00), the significant wave height reached more than 4 m offshore and still as high as 2 m on the main beach of Gâvres. The wave breaking at the storm's peak occurs just on the seaward slope of the dike, which is partially submerged depending on the sea level. An extraction of wave spectra and overall characteristics (left-hand portion of Fig. 3) was performed for the beach of Gâvres. At this point, the setup remains limited (less than 10 cm between 01:00 and 09:30, and nearly null, even a setdown at the storm peak, owing to the wave breaking on the dike). The analysis of the total sea level (tide, storm surge and wave setup) confirms that no overflowing appears and that the flood is caused only by wave overtopping.

The maxima of sea level and of wave heights are simultaneous (about 05:00), and the wave periods increase between 05:00 and 07:00, showing increasing wave energy and a potential for continued overtopping even if the sea level decreases. However, it is not possible to identify the time when the flooding starts and stops. For this reason, dynamic evolutions of sea level and wave characteristics need to be taken as an input in the overtopping and flood simulation.

3.3 Modelling wave overtopping and flood: model and inputs

3.3.1 The SURF-WB model

The site of Gâvres lies in a macro-tidal context. Consequently, the duration of the wave overtopping is mainly controlled by the tide, coupled with the storm surge and the

waves' evolutions. For this reason, the chosen model must be robust and stable enough to allow for sea-level variations of several meters during the tide.

The flooding was simulated using the time-dependent phase-resolving model SURF-WB in 2-D in view of its particular robustness. This model is based on the viscous NLSW equations, including several physical aspects with mathematical rigor: diffusion terms, friction terms, Coriolis effect, surface tension terms and wet/dry interface and dynamic time step (Marche et al., 2007). SURF-WB uses shock-capturing schemes to correctly represent the propagation of waves in the inner surf zone, and well-balanced schemes to deal with steep slopes. These specificities make SURF-WB particularly efficient for overtopping and urban flooding simulations. SURF-WB has formerly been used by Pedreros et al. (2011), in a micro-tidal context, to simulate coastal flooding in stationary conditions.

SURF-WB does not explicitly deal with energy dissipation by wave breaking. Nevertheless, several authors (Bonneton, 2007; Brocchini and Dodd, 2008; Kobayashi et al., 1989; Marche et al., 2007; etc.) have shown that the use of the NLSW equations with shock-capturing schemes could provide a correct representation of the waves after breaking: the energy dissipation is directly deduced from the shocks theory (Stocker, 1957), and even if the wave shapes are not reliable in the breaking zone, the results are quite similar to benchmarking results beyond the breaking zone (Tissier et al., 2012).

For Gâvres, SURF-WB has been implemented with a forcing very close to the coast (about 100 m), which makes it possible to reduce the classical problems caused by the absence of frequency dispersion in NLSW models (premature wave decrease, no shoaling, etc.): during the overtopping period, the sea level is quite high, and wave breaking is controlled by the steep slope of the dike; as waves are generated very close to the dike, they do not have enough time to significantly incur the effects of these constraints, and the energy dissipation occurs mainly on the dike. Moreover, a forcing very close to the coast offers the advantage of using quite homogeneous waves perpendicular to the coast (after refraction).

3.3.2 Forcing conditions for SURF-WB

The forcing condition for SURF-WB was imposed on the south-western boundary of the calculation area (represented at Fig. 2). SURF-WB does not use any wavemaker, but calculates the incoming fluxes to correctly reconstitute a time series for water level, at shallow depth. This implies that the waves have to be homogeneous along the forcing boundary and parallel to this boundary, which strongly constrains the domain limits according to the configuration of the coast. For the application in Gâvres, as the forcing boundary is very close to the dike (100 m), the waves have still refracted and are quite perpendicular to the coast and homogeneous along the boundary.

The model was forced with a time series of water-levels including both sea-level variations (tide and storm surge) and waves. This time series was established by extracting the sea level (including the tide, the storm surge and the wave setup at the extraction point) and the wave spectrum from the SWAN results, with a 10 min time step; this was used to reconstitute, using the DIWASP tool (Johnson, 2002), a random water-level series conform with the spectra (condition varying every 10 min), with a time step of 0.1 s. The time series generated covers from 02:40 to 08:00, to be sure to include the onset and the end of the overtopping. It is represented on the right-hand portion of Fig. 5.

This whole time series was imposed on the left boundary of the calculation area, and SURF-WB then calculated both wave propagation, overtopping and flood dynamics. Using single processor, the time computation is such that 5.3 h (with a time step of 0.043 s) are simulated in 8.5 days.

3.3.3 The digital elevation model

To simulate the flooding at a very high resolution, precise data are needed for topography and land use. This type of data is provided thanks to recent advances in airborne scanner laser altimetry (LiDAR), which is available on the studied site. Current processing makes it possible to obtain a precise and reliable Digital Terrain Model (DTM), but that lacks data on land use: buildings, walls, vegetation, etc. It is therefore necessary to

build a Digital Elevation Model (DEM) by extracting, from raw data, the largest possible amount of information about all the elements that interfere with the flooding, especially buildings and garden walls. The resolution of this DEM has to be sharp enough to correctly represent the water flows in the urban area, and assess all the potential pathways for water (Fewtrell, 2011).

For Gâvres, the LiDAR data characterization in terms of land use was procured semi-automatically with LasTools software (Hug et al., 2004), completed by a field survey. The DEM interpolation was performed with ArcGIS, with a 1 m resolution, and includes all buildings and walls in the studied area. Ultimately, the 1 m resolution grid numbers 607 nodes (from south-east to north-west) by 663 nodes (from north-east to south-west). It is important to note that, as the collapse time of the wall over the dike is still unknown, this wall has been considered as destroyed since the beginning of the simulation. Particular care has been taken with the representation of the dike and this wall, insofar as their topography strongly constrains the overtopping volume of water. This DEM is represented on Fig. 2.

3.3.4 The roughness map

Given the flooding configuration in Gâvres (filling of a topographic depression), the effect of the soil roughness is quite limited (essentially impacting the flow speeds), aside from the land–sea interface (dike and walls). It therefore was decided to distinguish only the natural sea floor (Manning coefficient of $0.025\,\mathrm{s\,m^{-1/3}}$, typical for gravels and natural channels), the concrete areas (dike and urban area including buildings, Manning coefficient of $0.014\,\mathrm{s\,m^{-1/3}}$) and the football pitch (Manning coefficient of $0.07\,\mathrm{s\,m^{-1/3}}$, typical for grass in built-up areas).

4 Model results: validation and analysis

4.1 Validation

The elements of validation are mainly the water height measurements of Cariolet (2010), the water stagnation area reported by Le Cornec and Peeters (2008), the locations of flooded houses and reports about the flood chronology.

4.1.1 Overtopping sectors

According to the simulation, most of the wave overtopping occurred in the "Beach street" and on the eastern part of the "Main Beach" dike, where the wall was destroyed. Between these two sectors, the overtopping remained rare and very limited. This can be observed on Fig. 7 that represents the water height on four numerical gauges in Gâvres: frequent wave overtopping can be underlined on Gauges 1 ("Beach street") and 3 ("Main Beach" dike), whereas overtopping remains sporadic and brief on Gauge 2. This is coherent with Cariolet (2010), who did not identify this sector as an overtopping zone (Fig. 8).

4.1.2 Extent of flooding

The water stagnation area indicated by the municipality lies totally within the flooded area indicated by the simulation. When compared to insured damages, the results are very coherent too, with all the concerned houses being included in the simulated flooded area (aside from the two northernmost points, supposed to have been affected by only a little water in the underground level, possibly due to waves coming directly from the north). A few houses west of the area, as well as others in the northernmost sector, were not indicated as having incurred damages, although the simulation indicates that these areas could be affected by several tens of centimetres of water.

4.1.3 Water heights

The 23 measurements made by Cariolet (2010) were performed after the event, mainly on the strength of marks left on the walls or the ground; it is consequently likely that these levels do not represent the maximum water height, but the levels at which the water stagnated. Moreover, they are quite difficult to interpret insofar as they are expressed directly in water height, with no reference made to the point where it was measured (micro-topography, interior or exterior of a house, etc.). These measurements also differ locally from the municipality's data and from the topography, in particular near the square located in the western part of the football pitch. For these reasons, the measurements obtained by Cariolet (2010) can be used to qualitatively validate the simulation.

Compared to the measurements (Fig. 9), the maximum or final water heights from the simulation are globally coherent. Taking into account the aforementioned limits, calculated maximum water heights are compatible with the measured values for 50 % of the points. The differences in water height do not exceed 10 cm for 60 % of cases, and 15 cm for 75 %. However, a couple of points in the middle of the area seem to be contradictory as compared to the simulation, reports (damage, stagnation area) and topography. This problem can be ascribed to measurement errors and other sources of uncertainties.

4.1.4 Flood chronology

The report quoted by Le Cornec and Peeters (2008) was given by the resident of a house located on the "Parc des Sports" street, near Gauge 4 (Fig. 7). It indicates that there was no water until 04:50, and that the water first arrived from the south via the street at 05:00 and from the football pitch at 05:10. The level rose to reach 65 cm inside the house between 05:30 and 05:45. A photograph taken at 06:16 shows that the level rose further as compared to one taken at 05:46. Compared to the water height simulated on Gauge 4 (Fig. 7), this report is virtually compatible with the simulation,

although in the simulation the onset of the flood is slightly earlier (around 04:40), but its subsequent progression is very close to the report. In the simulation, the water arrives simultaneously from the street and the football pitch; it should be borne in mind that the simulation has considered that the wall on the dike was destroyed from the start of the simulation, which could explain this discrepancy.

Finally, the simulation proves to be quite coherent with the available validation data: the extent of the flooded area is consistent with the observation, the maximum simulated water heights are comparable to the measurements, and the chronology seems to be quite correct in the light of available reports.

4.2 Analysis: flooding dynamics, water levels and currents

The results obtained by simulation allow us to have access, for each point of the calculation grid and for each time step, to the water heights and flows both at sea and inland: the overtopping and flooding can therefore be described in detail for each wave, as illustrated on Fig. 6.

The results of the simulation show that the wave overtopping starts at about 03:20 in the southern portion of the area ("Beach street") and at about 03:40 on the dike per se. The overtopping continues to be significant until about 06:40, with a maximum occurring approximately just after 05:00. After 07:00, the water flow rate becomes slightly negative because the water tends to recede into the sea via the access to sea in "Beach street". This is illustrated on Fig. 8, which depicts the evolution of the overtopping water flow rate vs. time (estimated with time steps of 1 and 10 min to smooth the wave effects). Finally, at the end of the simulation (at about 08:00), the flooded area corresponds to a stable stretch of water inland (Fig. 9), with a water level very close to the maximum water level during the simulation (Fig. 10).

The analysis of numerical gauges implanted in the simulation allows the mechanisms of the flood to be identified (Fig. 7):

– Gauge 1 ("Beach street"): the shape of the water height curve can be explained by a local overflowing not detected by coastal MARS and SWAN simulations due to coarse resolutions: after a couple of instances of wave overtopping, the sea level reached this topographic level at 03:50; the waves could then come directly inland, and were perceptible on the gauge; the level subsequently decreased with the tide, with overflow ending at about 07:30, and no water remained at the end of the simulation.

– Gauge 2 (located behind the dike, south of the football pitch): this gauge indicates only sporadic transiting water between 04:15 and 06:00, with no accumulation; a few waves overtopped the dike at this level, and this water progressively flowed toward the lowest areas, as illustrated in Fig. 6.

– Gauge 3 (located behind the dike, at the edge of the football pitch, where the wall over the dike collapsed): as for Gauge 2, only transiting water was observed from 04:15 to 05:30 (but more intensive), but from 05:30 to 06:45 the global level has risen, linked to the filling of the topographic depression constituted by the football pitch (Fig. 6); few wave arrivals could then be individually detected, and the water stabilized around 0.29 m.

– Gauge 4 ("Parc des Sports" street; practically at the bottom of the topographic depression): at this point, no wave arrivals were detectable because water arrived by flowing from the streets and from the football pitch. The rate at which the depression filled varied, depending on the overtopping waves and on the link between water height and shape of the depression (the rate of fill slowed after 04:50 because the volume of water input required to elevate the water surface increased considerably). The stabilization of the water level around 06:45 shows the presence of stagnant water inland.

The comparison between the simulated maximum water heights (Fig. 10) and those obtained by Le Cornec and Peeters (2008) shows that the maximum water heights

obtained here seem to be quite a bit smaller, but more consistent with the available observations. In terms of maximum current speeds (Fig. 10), the dynamic simulation of each wave overtopping highlights the existence of areas just behind the dike where speeds are high, whereas the approach based on imposing mean overtopping discharges could not attain such high values, but rather, smoothed the flows in the overtopping area.

4.3 Discussion: sensitivity to the description of buildings and limitations of the method

4.3.1 Urban representation

The same flood simulation was conducted directly on the DTM, thus without taking the buildings and the walls explicitly into account. The urbanized area has been represented through an increased soil roughness (Manning coefficient of $0.1\,\mathrm{s\,m}^{-1/3}$), and the dike and the football pitch are the only remaining unmodified elements (presence of the wall on the dike where it did not collapse, Manning coefficients of $0.014\,\mathrm{s\,m}^{-1/3}$ for concrete and $0.07\,\mathrm{s\,m}^{-1/3}$ for grass). The forcing condition is exactly the same as for the previous simulation (sea level and waves).

The results obtained (Fig. 11) show that, for the studied case of Gâvres where the flooding process remains quite slow (only overtopping and water flowing and filling a topographic depression), this type of representation of urbanization leads to results that are very similar to those obtained with a DEM (represented on Fig. 10). This is particularly true for the extension of the flooded area and for the maximum water heights.

Some significant differences, however, do appear between the two configurations in terms of flood dynamics. Indeed, as the flow speeds in the simulations are directly controlled by soil roughness, the flows are notably slower with an urbanized area represented by a high Manning coefficient than they are with an explicit representation of buildings, which can have significant consequences for hazard analysis in urban

areas. A comparison of the maximum calculated flow speeds in the two configurations (Fig. 12) shows that the differences are concentrated mainly on three sectors: the buildings (because they remain dry with the DEM); the main streets (here the "Parc des Sports" street), where an increased roughness leads to a significant underestimation of the current speeds (here from 1 to 2.5 m s^{-1} with the DEM to 0.2 to 0.3 m s^{-1} with an urban area represented by an increased roughness); and the seaside, where the high velocity area is directly limited by the identification of the urban area boundary and the associated transition in roughness coefficients.

Finally, this comparison shows that studying flooding in an urban area implies necessarily a realistic representation of the buildings in order to allow a precise interpretation of the results.

4.3.2 Limitations of the method

The use of time-dependent phase resolving models remains recent, and currently quite difficult to implement because of a certain number of limitations and difficulties.

The main limitations, directly linked to the numerical models, involve the physical processes taken into account; indeed, if wave breaking is now increasingly integrated into this type of model, the integration of erosion and breaching in dunes or dikes continues to date to be very problematical, despite the fact that these phenomena constitute a major explanation for many of coastal floods. The numerical approaches with respect to physical phenomena can constitute another limitation for these models, mainly concerning the forcing conditions, which need to be reliable enough to correctly generate the waves, with a robustness of the model that is sufficient to cope with general sea level evolution throughout a long simulation under non-stationary conditions.

Moreover, simulating overtopping and flooding at a very high resolution implies using very short time steps (largely higher than 10–20 Hz), which result in long calculation times, especially if the model used is not parallelized.

Finally, despite its efficiency, this type of simulation is still quite rare and expensive, due to the difficulty in implementing the time-dependent phase-resolving model

(optimization of the link between model limits and site configuration) and to the calculation time. For this reason, it remains currently restricted to urban areas with large assets or in the framework of research projects.

5 Conclusions

The goal of this study was to propose and apply a methodology able to simulate the whole complexity of the problem of a coastal flood by wave overtopping in an urban area. The proposed method relies on simulations on regional to local scales to calculate the evolution of sea level (tide and storm surge) and of wave characteristics, which are used to force a time-dependent phase-resolving model, using well-balanced shock-capturing schemes, in order to simulate wave overtopping. Moreover, the choice of such a model combined with the use of a very high resolution DEM (including buildings and walls) makes it possible to simulate at the same time the flood propagation in an urban area.

Finally, this approach enables the most important parameters of the phenomena to be taken into account: time evolution of sea level and wave characteristics (to simulate dynamically the time evolution of the event), spatial and temporal distribution of the overtopping and flood simulation in an urban area with explicit buildings.

This methodology has been applied to the site of Gâvres (Brittany, France), flooded during the Johanna storm in 2008. The SURF-WB model allowed this event to be reconstituted with a satisfactory level of precision compared to the available observations (flooded area, chronology, maximum water height).

A comparison of these results with a similar simulation using a more classical approach (no explicit buildings and walls, but an increased roughness for the whole urban area) showed the advantage of an explicit representation of buildings and walls for hazard assessment in urban areas: even if, in the particular case of Gâvres, the water height is not modified significantly by the simpler approach, the flood dynamics and

the current speeds are underestimated considerably in the streets and on the seafront when the effects of buildings are not explicitly integrated.

This type of simulation may, in the years to come, be increasingly called upon, thanks to the recent and future improvements of time-dependent phase-resolving models. However, the use of these models continues at present to be quite difficult due to a certain number of limitations and difficulties, mainly involved with physical processes (wave breaking, erosion and breaching, etc.), forcing conditions (wave generator, etc.) and computing time. Nevertheless, the constant progress being made in computing and numerical modelling should in fruition enable these limits to be overcome, thereby opening the way towards a generalization of these applications for operational studies.

References

André, C.: Analyse des dommages liés aux submersions marines et évaluation des coûts induits aux habitations à partir de données d'assurance, perspectives apportées par les tempêtes Johanna (2008) et Xynthia (2010), Ph.D. thesis, University of Western Brittany, Brest, 2013 (in French).

André, C., Monfort, D., Bouzit, M., and Vinchon, C.: Contribution of insurance data to cost assessment of coastal flood damage to residential buildings: insights gained from Johanna

(2008) and Xynthia (2010) storm events, Nat. Hazards Earth Syst. Sci., 13, 2003–2012, doi:10.5194/nhess-13-2003-2013, 2013.

Ardhuin, F., Rogers, A., Babanin, A., Filipot, J. F., Magne, R., Roland, R., Westhuysen, A. V. D., Queffleulou, P., Lefevre, L., Aouf, L., and Collard, F.: Semi-empirical dissipation source functions for ocean waves: Part I, definition, calibration and validation, J. Phys. Oceanogr., 40, 1917–1941, 2010.

Bates, P. D. and De Roo, A. P. J.: A simple raster-based model for flood inundation simulation, J. Hydrol., 236, 54–77, 2000.

Bates, P. D., Dawson, R. J., Hall, J. W., Horritt, M. S., Nicholls, R. J., Wicks, J., and Hassan, M. A. A. M.: Simplified two-dimensional numerical modeling of coastal flooding and example applications, Coast. Eng., 52, 793–810, 2005.

Bates, P. D., Horitt, M. S., and Fewtrell, T. J.: A simple inertial formulation of the shallow water equations for efficient two dimensional flood inundation modeling, J. Hydrol., 387, 33–45, 2010.

Begnudelli, L., Sanders, B. F., and Bradford, S. F.: An adaptive Godunov-based model for flood simulation, J. Hydraul. Eng., 134, 714–725, 2008.

Bonneton, P.: Modelling of periodic wave transformation in the inner surf zone, Ocean Eng., 34, 1459–1471, 2007.

Bonneton, P., Chazel, F., Lannes, D., Marche, F., and Tissier, M.: A splitting approach for the fully nonlinear and weakly dispersive Green-Naghdi model, J. Comput. Phys., 230, 1479–1498, 2011.

Booij, N., Ris, R. C., and Holthuijsen, L. H.: A third-generation wave model for coastal regions, Part I, model description and validation, J. Geophys. Res., 104, 7649–7666, 1999.

Breilh, J. F., Chaumillon, E., Bertin, X., and Gravelle, M.: Assessment of static flood modeling techniques: application to contrasting marshes flooded during Xynthia (western France), Nat. Hazards Earth Syst. Sci., 13, 1595–1612, doi:10.5194/nhess-13-1595-2013, 2013.

Brocchini, M. and Dodd, N.: Nonlinear shallow water equation modeling for coastal engineering, J. Waterw. Port C.-ASCE, 134, 104–120, 2008.

Cariolet, J.-M.: Use of high water marks and eyewitness accounts to delineate flooded coastal areas: the case of Storm Johanna (10 March 2008) in Brittany, France, Ocean Coast. Manage., 53, 679–690, 2010.

Cariolet, J.-M.: Inondation des côtes basses et risques associés en Bretagne, Ph.D. Thesis of the University of Western Brittany, Brest, 2011 (in French).

Cariolet, J.-M., Costa, S., Caspar, R., Ardhuin, F., Magne, R., and Goasguen, G.: Atmospheric and marine aspects of the 10 March 2008 storm in Atlantic and in the Channel, Norois, 215, 11–31, doi:10.4000/norois.3242, 2010 (in French).

Fewtrell, T. J., Duncan, A., Sampson, C. C., Neal, J. C., and Bates, P. D.: Benchmarking urban flood models of varying complexity and scale using high resolution terrestrial LiDAR data, Phys. Chem. Earth, 36, 281–291, 2011.

Fortunato, A. B., Rodrigues, M., Dias, J. M., Lopes, C., and Oliveira, A.: Generating inundation maps for a coastal lagoon: a case study in the Ria de Aveiro (Portugal), Ocean Eng., 64, 60–71, 2013.

Gallegos, H. A., Schubert, J. E., and Sanders, B. F.: Two-dimensional, high-resolution modeling of urban dam-break flooding: a case study of Balwin Hills, California, Adv. Water Resour., 32, 1323–1335, 2009.

Gallien, T. W., Schubert, J. E., and Sanders, B. F.: Predicting tidal flooding of urbanized embayments: a modeling framework and data requirements, Coast. Eng., 58, 567–577, 2011.

Hug, C., Krzystek, P., and Fuchsc, W.: Advanced LiDAR data processing with LasTools, XXth ISPRS Congress, 12–23. July 2004, Istanbul, Turkey, 2004.

Johnson, D.: DIWASP: DIrectional WAve SPectra Toolbox, Version 1.1: User Manual, Research Report No: WP 1601 DJ (V1.1), Coastal Oceanography Group Centre for Water Research, University of Western Australia, Perth, 2002.

Kobayashi, N., Silva, G. D., and Watson, K.: Wave transformation and swash oscillation on gentle and steep slopes, J. Geophys. Res. 94, 951–966, 1989.

Lannes, D. and Marche, F.: A new class of fully nonlinear and weakly dispersive Green-Naghdi models for efficient 2-D simulations, J. Comp. Phys., submitted, 2014.

Lazure, P. and Dumas, F.: An external-internal mode coupling for a 3-D hydrodynamical model for applications at regional scale (MARS), Adv. Water Resour., 31, 233–250, doi:10.1016/j.advwatres.2007.06.010, 2008.

Le Cornec, E. and Peeters, P.: Simulation de la tempête du 10 mars 2008 sur le site de la Grande Plage de Gâvres, Rapport d'étude GEOS-DHI, 2008 (in French).

Le Roy, R. and Simon, B.: Réalisation et validation d'un modèle de marée en Manche et dans le Golfe de Gascogne. Application à la réalisation d'un nouveau programme de réduction des sondages bathymétriques, EPSHOM (Etablissement Principal du Service Hydrographique et Océanographique de la Marine, Brest), Technical report no 002/03, 2003, 2003 (in French).

Lynett, P. J.: Nearshore wave modeling with high-order Boussinesq-type equations, ASCE Journal of Waterway, Port, Coast. Ocean Eng., 132, 348–357, 2006.

Lynett, P. J., Melby, J. A., and Kim, D. H.: An application of Boussinesq modeling to Hurricane wave overtopping and inundation, Ocean Eng., 37, 135–153, 2010.

Marche, F., Bonneton, P., Fabrie, P., and Seguin, N.: Evaluation of well-balanced bore-capturing schemes for 2d wetting and drying processes, Int. J. Numer. Meth. Eng., 53, 867–894, 2007.

McCabe, M. V., Stansby, P. K., and Apsley, D. D.: Random wave runup and overtopping a steep sea wall: shallow-water and Boussinesq modelling with generalised breaking and wall impact algorithms validated against laboratory and field measurements, Coast. Eng., 74, 33–49, 2013.

Neal, J. C., Bates, P. D., Fewtrell, T. J., Hunter, N. M., Wilson, M. D., and Horritt, M. S.: Distributed whole city water level measurements from the Carlisle 2005 urban flood event and comparison with hydraulic model simulations, J. Hydrol., 368, 42–55, 2009.

Pedreros, R., Vinchon, C., Lecacheux, S., Delvallée, E., Balouin, Y., Garcin, M., Krien, Y., Le Cozannet, G., Poisson, B., Thiebot, J., Bonneton, P., and Marche, F.: Multi models approach to assess coastal exposure to marine inundation within a global change context, Poster, EGU (European Geosciences Union) General Assembly, Wien, 3–4 April 2011, 2011.

Peeters, P., Schoorens, J., Lecornec, E., Michard, B., and Lechat, M.: Définition de l'aléa submersion marine sur le site de la Grande Plage de Gâvres (Morbihan), La Houille Blanche, 1-2009, 45–51, doi:10.1051/lhb:2009004, 2009 (in French).

Saha, S., Moorthi, S., Pan, H.-L., Wu, X., Wang, J., Nadiga, S., Tripp, P., Kistler, R., Woollen, J., Behringer, D., Liu, H., Stokes, D., Grumbine, R., Gayno, G., Wang, J., Hou, Y.-T., Chuang, H.-Y., Juang, H.-M. H., Sela, J., Iredell, M., Treadon, R., Kleist, D., Van Delst, P., Keyser, D., Derber, J., Ek, M., Meng, J., Wei, H., Yang, R., Lord, S., Van Den Dool, H., Kumar, A., Wang, W., Long, C., Chelliah, M., Xue, Y., Huang, B., Schemm, J.-K., Ebisuzaki, W., Lin, R., Xie, P., Chen, M., Zhou, S., Higgins, W., Zou, C.-Z., Liu, Q., Chen, Y., Han, Y., Cucurull, L., Reynolds, R. W., Rutledge, G., and Goldberg, M.: The NCEP Climate Forecast System Reanalysis, B. Am. Meteorol. Soc., 91, 1015–1057, doi:10.1175/2010BAMS3001.1, 2010.

Schubert, J. E. and Sanders, B. F.: Building treatments for urban flood inundation models and implications for predictive skill and modeling efficiency, Adv. Water Resour., 41, 49–64, 2012.

Schubert, J. E., Sanders, B. F., Smith, M. J., and Wright, N. G.: Unstructured mesh generation and landcover-based resistance for hydrodynamic modeling of urban flooding, Adv. Water Resour., 31, 1603–1621, 2008.

Shi, F., Kirby, J. T., Harris, J. C., Geiman, J. D., and Grilli, S. T.: A high-order adaptive time-stepping TVD solver for Boussinesq modeling of breaking waves and coastal inundation, Ocean Model., 43–44, 36–51, doi:10.1016/j.ocemod.2011.12.004, 2012.

SHOM: Références Altimétriques Maritimes, Ports de France métropolitaine et d'outre-mer, Cotes du zéro hydrographique et niveaux caractéristiques de la marée, Service Hydrographique et Océanographique de la Marine (Brest), ISBN 978-2-11-097286-6, 2012 (in French).

Smith, R. A. E., Bates, P. D., and Hayes, C.: Evaluation of coastal flood inundation model using hard and soft data, Environ. Model. Softw., 30, 35–46, 2012.

Stocker, J. J.: Water Waves – the Mathematical Theory With Applications, Interscience Publishers, Inc., New York, 1957.

Tissier, M., Bonneton, P., Marche, F., Chazel, F., and Lannes, D.: A new approach to handle wave breaking in fully non-linear Boussinesq models, Coast. Eng., 67, 54–66, doi:10.1016/j.coastaleng.2012.04.004, 2012.

Tonelli, M. and Petti, M.: Numerical simulation of wave overtopping at coastal dikes and low-crested structures by means of a shock-capturing Boussinesq model, Coast. Eng., 79, 75–88, 2013.

Torres-Freyermuth, A., Mariño-Tapia, I., Coronado, C., Salles, P., Medellín, G., Pedrozo-Acuña, A., Silva, R., Candela, J., and Iglesias-Prieto, R.: Wave-induced extreme water levels in the Puerto Morelos fringing reef lagoon, Nat. Hazards Earth Syst. Sci., 12, 3765–3773, doi:10.5194/nhess-12-3765-2012, 2012.

van der Meer, J. W.: Technical Report Wave Run-up and Wave Overtopping at Dikes, TAW/Technical Advisory Committee on Flood Defense, Delft, 2002.

Zijlema, M., Stelling, G., and Smit, P.: SWASH: an operational public domain code for simulating wave fields and rapidly varied flows in coastal waters, Coast. Eng., 58, 992–1012, doi:10.1016/j.coastaleng.2011.05.015, 2011.
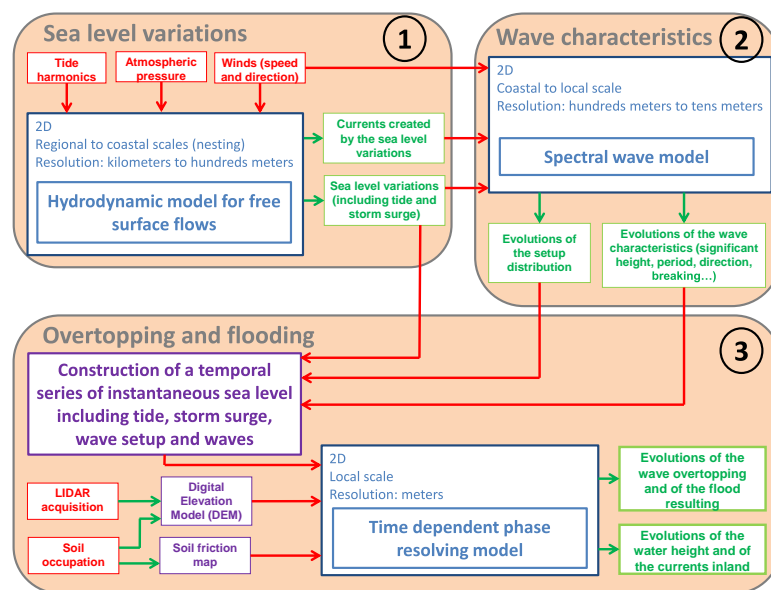
Figure 1. Modelling method proposed to simulate wave overtopping and associated flooding.

Figure 2. Location map of Gâvres, areas covered by the simulations and main overtopping mechanisms during the Johanna storm.

4975
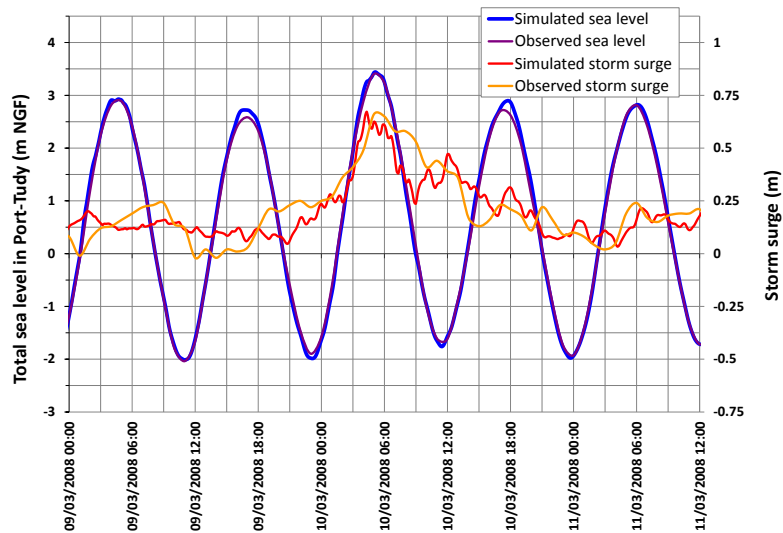
Figure 3. Validation of the total sea level (tide and storm surge) and of the storm surge simulated with MARS in Port-Tudy (observation from http://refmar.shom.fr).
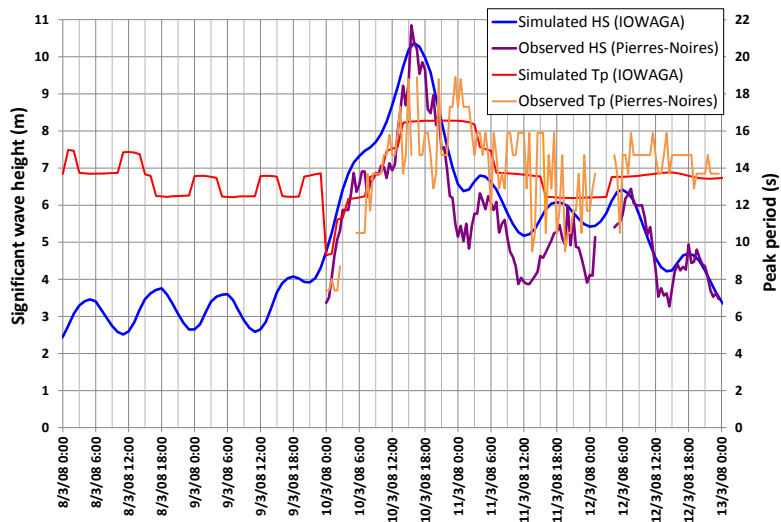
4976

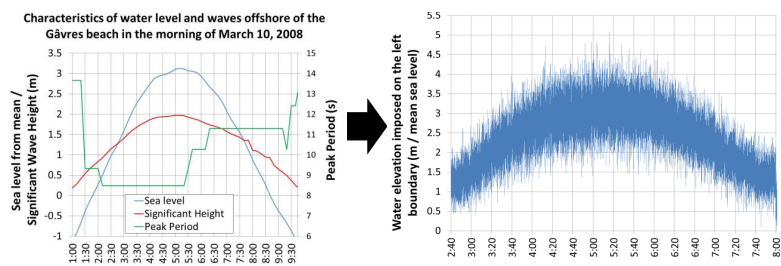**Figure 4.** Validation of the wave characteristics simulated in the IOWAGA project on the Pierres-Noires gauge (observation from http://candhis.cetmef.developpement-durable.gouv.fr).

Figure 5. Evolution of the sea conditions near Gâvres during Johanna storm (sea level from MARS simulations, significant wave height and peak period from SWAN simulations) on the left, and reconstitution of a corresponding time series of water level with the DIWASP toolbox on the right.
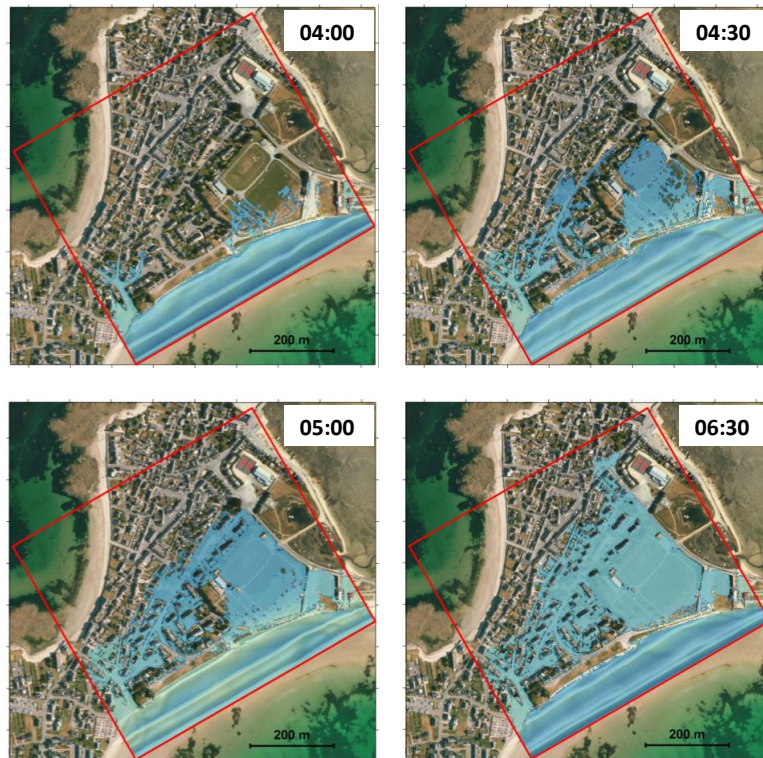
Figure 6. "Snapshots" of the SURF-WB simulation of overtopping and flooding: situation at 04:00, 04:30, 05:00 and 06:30 (UTC).
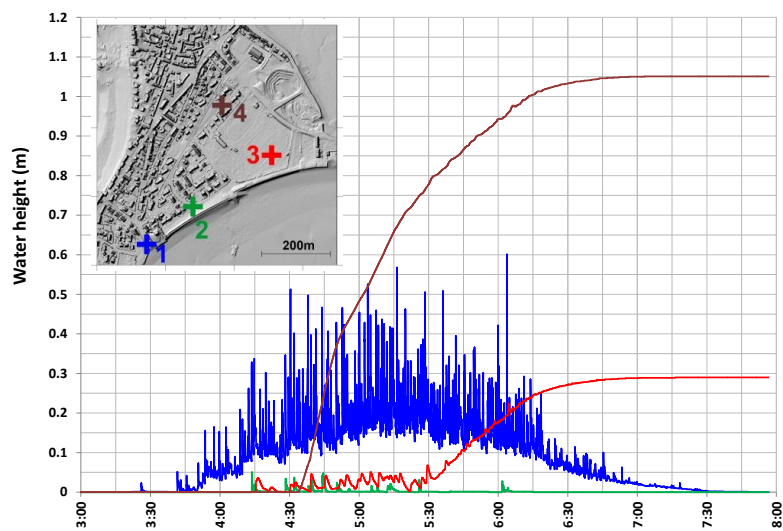
Figure 7. Evolution of the water height on four numerical gauges during the SURF-WB simulation on the DEM.
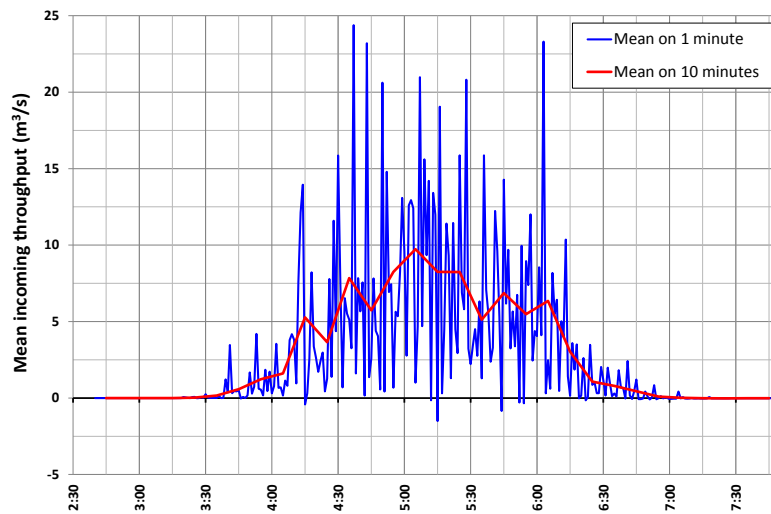
Figure 8. Evolution of the overtopping flow rate vs. time (estimated at the time steps of 1 and 10 min) during the SURF-WB simulation.
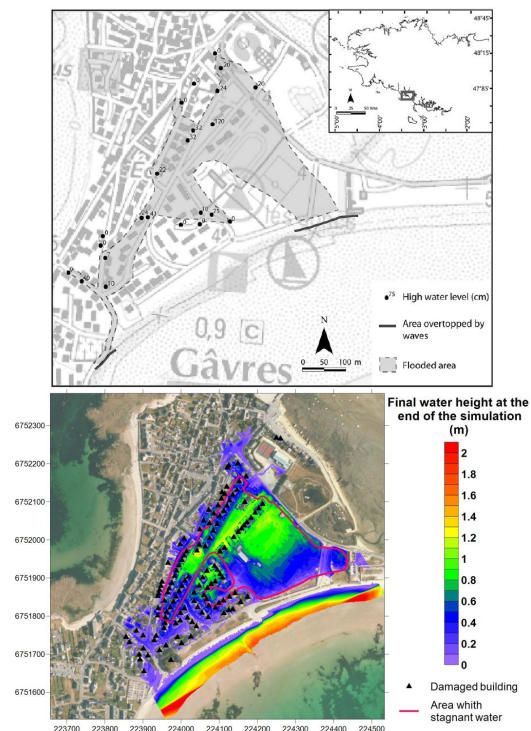
Figure 9. Above: measurements of maximum water heights (Cariolet, 2010); below: final water height at the end of the SURF-WB simulation and reported flooded buildings and stagnation area according to the municipality (from the Gâvres municipality and Le Cornec and Peeters, 2008).
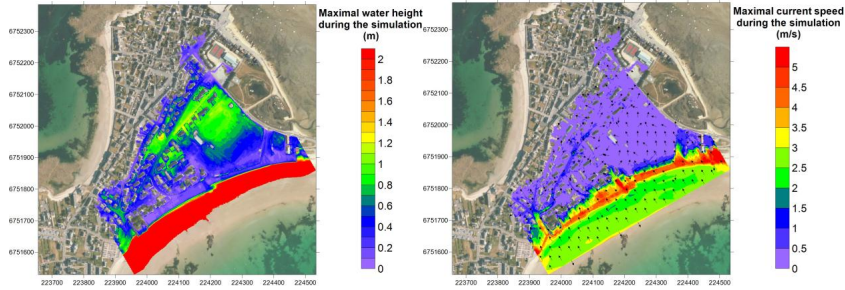
Figure 10. Maximum water heights (left) and currents (right) obtained inland during the SURF-WB simulation on the DEM (with explicit representation of the buildings).
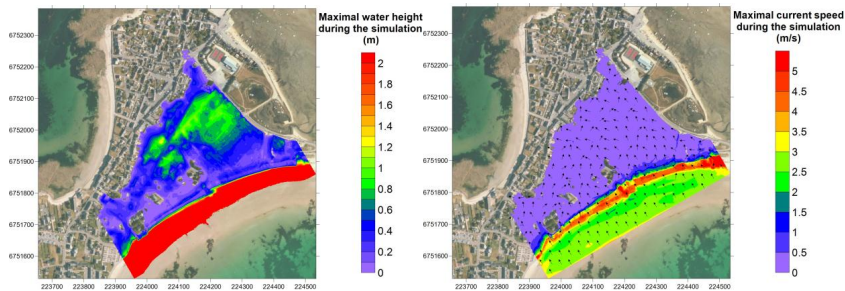
Figure 11. Maximum water heights (left) and currents (right) obtained inland during the SURF-WB simulation on the DTM (without explicit representation of the buildings).
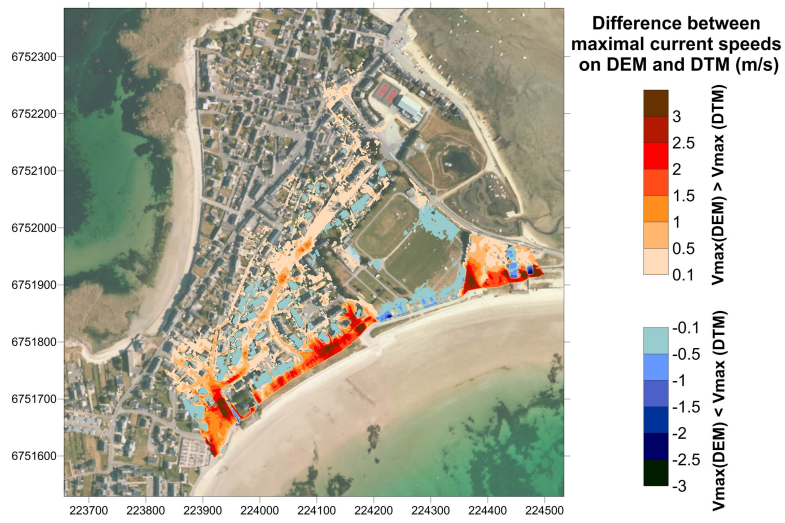
Figure 12. Difference between the maximum current speeds obtained inland during the SURF-WB simulations, with and without an explicit representation of the buildings ($V_{\text{max DEM}} - V_{\text{max DTM}}$).